Trajectory Control of a Linear Switched Reluctance Motor using a Two-Degree-of-Freedom Controller

S. W. Zhao, N. C. Cheung, *IEEE Member* and W. C. Gan, *IEEE Member*

Abstract **- Linear Switched Reluctance Motors (LSRMs) have been an attractive choice for direct-drive applications due to their low-cost and simple structures. However, LSRMs are difficult to control because of the highly nonlinear model. In this paper, a LSRM model, which takes the winding current tracking as a part of the LSRM model, is first proposed based on the two-time-scale method. According to this model, a basic yet effective two-degree-of-freedom controller is developed. The two-degree-of-freedom controller is as low cost as the conventional proportional-derivative (PD) controller but it has better the high frequency tracking capability than the conventional PD controller. Experimental results indicate that the LSRM model is effective for the controller design and the position tracking system with the proposed controller can track the position command accurately.**

Index terms –LSRM, simplified model of LSRM, position control, motor winding excitation scheme.

I. INTRODUCTION

In recent years, Linear Switched Reluctance Motors (LSRMs) have gained increasing attention because of their low-cost, simple structures and the ability of operating in some harsh conditions. Compared to the method of rotary motors with transformation components to produce linear motion, LSRMs have many advantages, such as quickly response, high sensitivity and tracking capability, moreover the structure of LSRMs can reduce the room needed for its installation. These advantages make LSRMs an attractive choice for direct-drive applications. However, LSRMs are difficult to control and their outputs have high force ripples because mathematical models of LSRMs are highly dependent on their complex magnetic circuits which are difficult to model, simulate and control.

Switched Reluctance Motors (SRMs) have been explored from different aspects in [1-6]. A control drive system for SRMs has been presented in [6]. In [7], a method of torque ripple minimization for SRMs has been discussed. Force distribution functions, force and current control of LSRMs have been presented in [8-11]. A precise position control scheme for LSRMs can be found in [9, 11 and 12]. In [9], the authors proposed a simple yet effective position controller using a look-up table and a robust compensator. A closed form solution for nonlinear current-position-current model is further developed in [12].

The work is supported by the Hong Kong Polytechnic University Research Grants Council under the project code BQ831.

S. W. Zhao and N. C. Cheung are with Department of Electrical Engineering, Hong Kong Polytechnic University, Hunghom, Hong Kong SAR, China. (Corresponding author: N. C. Cheung, e-mial: eencheun@polyu.edu.hk).

W. C. Gan is with Motion Group, ASM Assembly Automation Hong Kong Ltd., Kwai Chung, Hong Kong SAR, China (e-mail: wcgan@asmpt.com).

In paper, the two-time-scale analysis method is applied in the LSRM system for modeling. Generally the dynamics of the mechanical position is much slower than that of the electrical current. When the mechanical variables are mainly discussed, the electromagnetic variables can be regards as constants. Therefore, a LSRM model which takes winding current tracking as a part of LSRM model is proposed here. The conventional proportional-derivative (PD) controller is often used in position servo system for its low-cost, easy realization and good stability. However, its performance would deteriorate quickly for high frequency signal. Based the model a two-degree-of-freedom position controller is developed for the LSRM. Compared with the conventional PD controller, the proposed controller has better tracking ability for high frequency signal. The experimental results demonstrate the effectiveness of the proposed model and controller.

The organization of this paper is as follows. The construction and the modeling of the LSRM are given in section II. The position controller design is introduced in section III. In section IV, the experimental results are presented. Finally, conclusions are given in section V.

II. CONSTRUCTION AND MODELING OF THE LSRM

A. CONFIGURATION OF THE LSRM

A set of three-phase coils is installed on the moving platform as shown in Fig. 1. The three coils are with the same dimensions. The body of the moving platform is manufactured with aluminum, so that the total weight of the moving platform and its inertia are low and the magnetic paths are decoupled. The stator track and the core of the windings are laminated with 0.5mm silicon-steel plates. Table 1 depicts the electrical and mechanical parameters of the LSRM. A 0.5um resolution linear optical encoder is integrated in the LSRM system to observe the motion profile of the moving platform and provides the feedback position information.

A set of three-phase coils is installed on the moving platform as shown in Fig. 1. The three coils are with the same dimensions. The body of the moving platform is manufactured with aluminum, so that the total weight of the moving platform and its inertia are low and the magnetic paths are decoupled. The stator track and the core of the windings are laminated with 0.5mm silicon-steel plates. Table 1 depicts the electrical and mechanical parameters of the LSRM. A 0.5um resolution linear optical encoder is integrated in the LSRM system to observe the motion profile of the moving platform and provides the feedback position information.

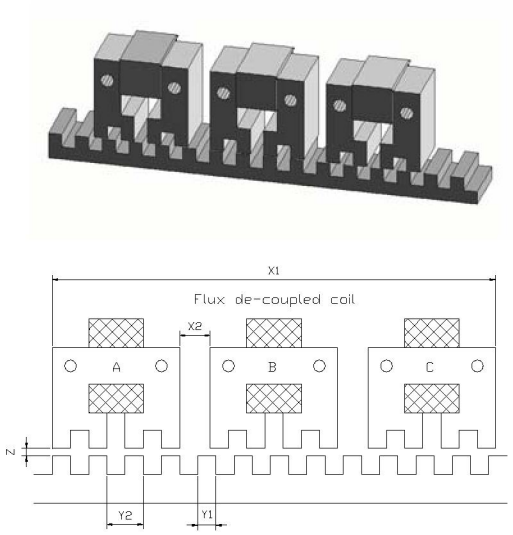

Fig. 1: Schematic of the LSRM.

Table 1
THE ELECTRICAL AND MECHANICAL PARAMETERS OF THE LSRM

Pole width (y_1)	6mm
Pole pitch (y_2)	12mm
Phase separation (x_2)	10mm
Winding length (x_3)	30mm
Wind width (l)	25mm
Air gap width (z)	0.5mm
Phase resistance	2.5 Ω
Aligned inductance	19.2mH
Unaligned inductance	11.5mH
Mass of the moving platform (M)	1.8Kg
Friction constant (B)	0.08N*s*m^{-1}

B. MODELING OF THE LSRM

The switched reluctance linear drive system has a highly nonlinear characteristic. The nonlinear mathematical model of the LSRM can be described by voltage balancing equations (1) and force balancing equation of the moving platform (2) and (3), as follows

$$v_j = r_j i_j + \frac{d\lambda_j}{dt}, j = a,b,c. \quad (1)$$

$$f_e = \sum_{j=a}^{c} \frac{\partial \int_0^{i_j} \lambda_j di_j}{\partial x}. \quad (2)$$

$$f_e = M\frac{d^2x}{dt^2} + B\frac{dx}{dt} + f_l. \quad (3)$$

where v_j is the voltage applied to the terminals of phase j, i_j is the current of phase j, r_j is the winding resistance and λ_j is the phase flux linkage of phase j, x is the displacement, f_e is the generated electromagnetic force, f_l is the external load force, M and B are the mass and friction constants respectively.

The mechanical part can be described by following equations, in which the external load force is not considered.

$$\frac{X(s)}{F_e(s)} = \frac{1}{(Ms+B)s}. \quad (4)$$

The phase electromagnetic force production equation can be approximated as (5),

$$f_j(x,i_j) = \frac{1}{2}\frac{dL_j}{dx}i_j^2, j = a,b,c \quad (5)$$

where f_j is the generated electromagnetic force of phase j, $\frac{dL_j}{dx}$ is the inductance change rate of phase j.

One characteristic of the LSRM is that it must be driven synchronously with its position. In general, the motor winding excitation scheme for LSRMs can be considered as a Force Distribution Function (FDF) and an approximated function of inductance change rate. The scheme of the driver can be shown as Fig. 2. The FDF is used to compute the force for each phase according to the position and the direction. The approximated function of inductance change rate is used to compute the phase current according to the command force of phase and the position. Some methods have been proposed for the approximated function of inductance change rate. They can be classified into two types: the type of look-up table and the type of approximated function. When the FDF and the approximated function of inductance change rate are chosen, the current can be computed by the inverse function (5) $f_j^{-1}(x,i_j)$ of equation with command force and its position. In this paper, the FDF is chosen as in table 2 [9] and the approximated function of inductance change rate is described as in (6) [2].

$$\frac{dL_j(x_j(t))}{dx_j(t)} = -K_{pj}\sin(\frac{2\pi x_j(t)}{y_2}), j = a,b,c$$
$$x_b = x_a + \frac{2y_2}{3} \quad . (6)$$
$$x_c = x_a + \frac{y_2}{3}$$

Here y_2, x_j and K_{pj} are the pole pitch of the LSRM, the displacement of phase j and a proportional parameter respectively.

Table 2 FORCE DISTRIBUTION FUNCTION (FDF) SCHEME.

Position range	+ force command	- force command
0mm-2mm	$f_B=f_x$	$f_C=0.5(2-x)f_x$, $f_A=0.5xf_x$
2mm-4mm	$f_B=0.5(4-x)f_x$, $f_C=0.5(x-2)f_x$	$f_A=f_x$
4mm-6mm	$f_C=f_x$	$f_A=0.5(6-x)f_x$, $f_B=0.5(x-4)f_x$
6mm-8mm	$f_C=0.5(8-x)f_x$, $f_A=0.5(x-6)f_x$	$f_B=f_x$
8mm-10mm	$f_A=f_x$	$f_B=0.5(10-x)f_x$, $f_C=0.5(x-8)f_x$
10mm-12mm	$f_A=0.5(12-x)f_x$, $f_B=0.5(x-10)f_x$	$f_C=f_x$

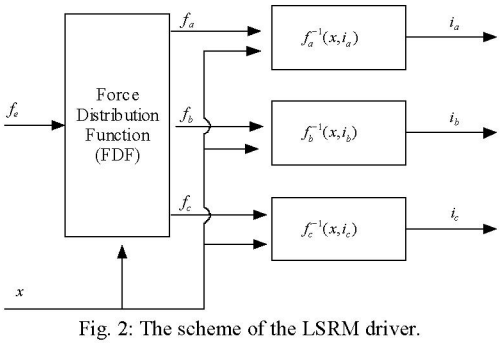

Fig. 2: The scheme of the LSRM driver.

According to the approximated function of inductance change rate (6) and the FDF in Table II, the output force experiment is performed on the proposed LSRM. The experimental data is shown in Fig. 3. It can be seen that the output force is found to increase with the command force and the change rate of output force is almost kept as a constant value. There are output force ripples at the same force command when the position changes.

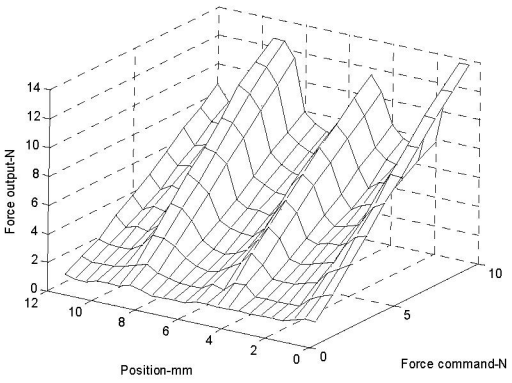

Fig. 3: Experimental force command vs position vs force output 3D chart.

The relationship between input force command f_i and output force f_o can be described as (7).

$$f_o = g(x) f_i, g(x) > 0 . \quad (7)$$

Here $g(x) f_i$ stands for the total electromechanical force, which represents the nonlinearity of LSRM in this model. Because the directions of input force command are always are the same with the directions of the output force, the relationship $g(x) > 0$ is always satisfied.

In general, the mechanical time constant is much slower than the electrical time constant of the current tracking loop [13]. Therefore, the two-time-scale analysis and design can be applied in the LSRM system. The dynamics of the mechanical position is slower than that of the electrical current. When the mechanical variables are mainly discussed, the electromagnetic variables can be regarded invariable. With the current tracking controller [8, 9], the current tracking part can be considered as a proportional part and the LSRM can be considered as a second-order system. If $g(x)$ is considered as a constant for a slowly changing position, the LSRM system can be described as (8),

$$\frac{X(s)}{F_i(s)} = \frac{g(x)}{(Ms+B)s}, g(x) > 0 . \quad (8)$$

III. CONTROLLER DESIGN FOR THE LSRM

According to the model, the LSRM is described as (8), which is a second order system, a PD controller is considered for the position tracking of the LSRM system. The control system is depicted in Fig. 4.

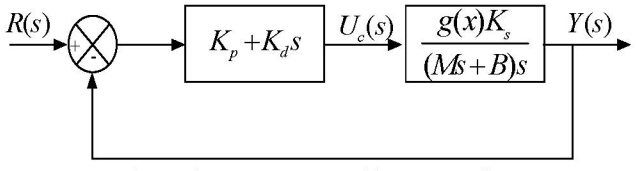

Fig. 4: The LSRM system with PD controller.

The closed loop transfer function is given in (9). Here K_p, K_d and K_s are proportional gain, differential gain of the controller and system gain respectively.

$$\frac{Y(s)}{R(s)} = \frac{g(x)K_s(K_p + K_d s)}{Ms^2 + (B + g(x)K_s K_d)s + g(x)K_s K_p} . \quad (9)$$

The error-input transfer function can be described as (10) in the low frequency band. As presented in (10), the error equation is a high pass filter and the error will increase quickly as the frequency of the input signal increases.

$$\frac{E(s)}{R(s)} = \frac{Ms^2 + Bs}{K_s K_p g(x)} . \quad (10)$$

To improve the performance of the controller, the position control system is proposed to control by a two-degree-of-freedom controller as shown in Fig. 5.

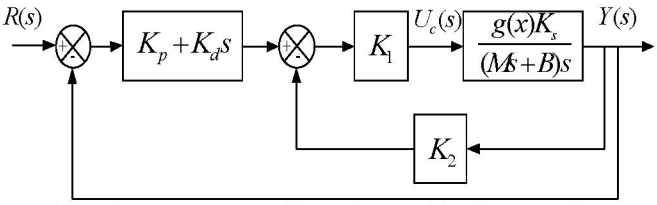

Fig. 5: The LSRM system with two-degree-of-freedom controller.

Then the system can be described as (11).

$$\frac{Y(s)}{R(s)} = \frac{g(x)K_s K_1(K_p + K_d s)}{Ms^2 + (B + K_d g(x)K_s K_1)s + g(x)K_s K_1(K_2 + K_p)} . \quad (11)$$

The error-input transfer function is given by the following equation.

$$\frac{E(s)}{R(s)} = \frac{Ms^2 + Bs + g(x)K_s K_1 K_2}{Ms^2 + (B + g(x)K_s K_1 K_d)s + g(x)K_s K_1(K_2 + K_p)} .$$

When $K_1 K_2$ is set at a proper value, the relationship $g(x)K_s K_1 K_2 >> Ms^2 + Bs$ can be satisfied in the low frequency band. Then the error equation is presented as (12) in the low frequency band, which is a low pass filter. The bandwidth increases with the increase of $K_1 K_2$. From (12), the error will decrease when the frequency of the input signal increases. The controller, therefore, has better tracking capability for high frequency signal than the conventional PD controller.

$$\frac{E(s)}{R(s)} = \frac{g(x)K_s K_1 K_2}{Ms^2 + (B + g(x)K_s K_1 K_d)s + g(x)K_s K_1(K_2 + K_p)} . \quad (12)$$

IV. EXPERIMENTAL RESULTS

A picture of the experimental setup is shown in Fig. 6.

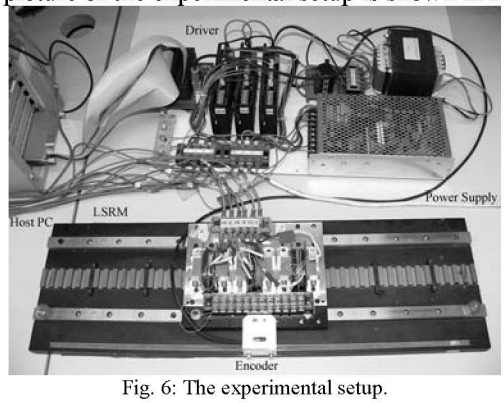

Fig. 6: The experimental setup.

The host PC is a Pentium 4 computer that is used to download the target code into a dSPACE DS1104 DSP motion controller card. The control algorithm is developed under the MATLAB/SIMULINK environment. All control functions are implemented by the DS1104 card, which is plugged into a PCI bus of the host PC. For the current tracking amplifier, the driver consists of three asymmetric bridge IGBT inverters with 90VDC voltage supplier. A linear optical encoder with 0.5um resolution is mounted on the mover of the LSRM system and provides position feedback information.

Fig. 7 shows the position response of square wave for the two-degree-of-freedom controller, while Fig. 8 shows the corresponding response for the PD controller. From the figures, both of the controllers can track the command wave accurately.

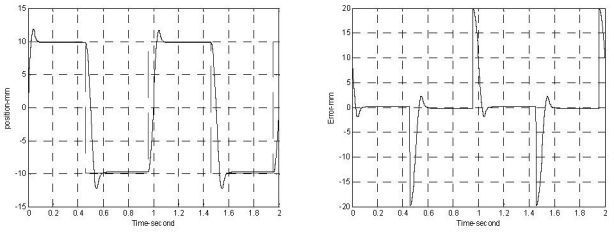

Fig. 7: Position response of square wave for the two-degree-of-freedom controller.

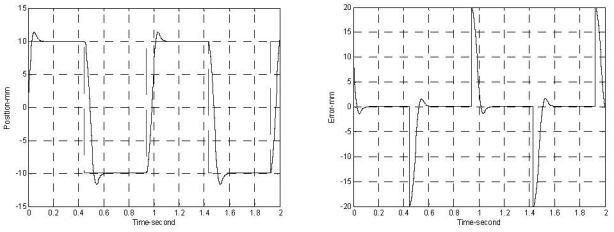

Fig. 8: Position response of square wave for the PD control.

Fig. 9 shows the position response of sinusoidal wave for the two-degree-of-freedom controller with frequency of input signal increasing, while Fig. 10 shows the one for the PD controller. As shown in Fig. 9, the maximum error for the two-degree-of-freedom controller decreases slowly as the frequency of input signal increases. However, the maximum error for the PD controller increases quickly from 0.2mm to 0.7mm as the frequency of the input signal increases in Fig. 10.

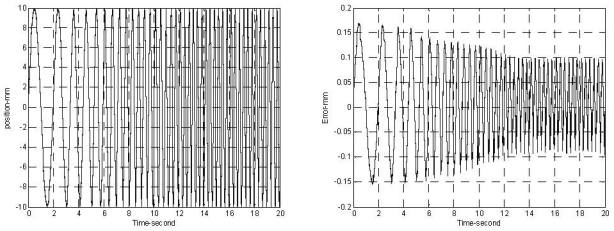

Fig. 9: Position response of sinusoidal wave for the two-degree-of-freedom controller with frequency of input signal increasing.

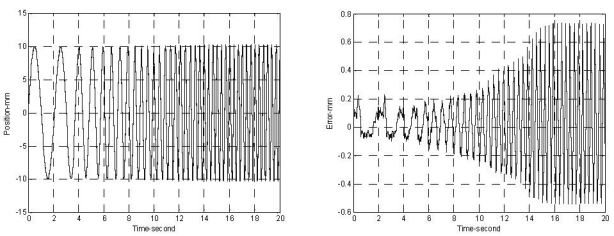

Fig. 10: Position response of sinusoidal wave for the PD controller with frequency of input signal increasing.

The experimental results demonstrate that the design of controllers based on the proposed model is effective. Both of the controllers can operate well. However, the two-degree-of-freedom controller can better track the high frequency signal than the conventional PD controller.

V. CONCLUSIONS

In this paper, the LSRM model and the controller for position tracking applications are discussed. Following contributions are made in this paper. (1) A LSRM model is obtained and the experimental results show its effectiveness. (2) A two-degree-of-freedom controller is designed for position tracking of LSRM system. The controller is as low cost as the conventional PD controller but it has a better tracking capability for high frequency signal than the PD controller. And the experimental results indicate the effectiveness of the model and the controller.

VI. REFERENCES

[1] T. J. E. Miller, *Switched Reluctance Motor and Their Control.* London, U. K.:Oxford Univ. Press, 1993.

[2] F. Khorrami, P. Krishnamurthy and H. Melkote, *Modeling and Adaptive Nonlinear Control of Electric Motors.* Germany: springer, 2003.

[3] U. S. Deshpande, J. J. Cathey and E. Richter, "High-force density linear switched reluctance machine," *IEEE Trans. Ind. Applicat.*, vol. 31, pp.345-352, Mar./Apr. 1995.

[4] B. S. Lee, H. K. Bae, P. Vijayraghavan and R. Krishnan, "Design of a linear switched reluctance machines," *IEEE Trans. Ind. Applicat.*, vol. 36, pp. 1571-1580, Nov./Dec. 2000.

[5] W. C. Gan, N. C. Cheung, "Design of a linear switched reluctance motor for high precision applications," in *IEEE International Electric Machines and Drives Conference (IEMDC 2001)*, 2001, pp.701-704.

[6] J. Borka, K. Lupan and L. Szamel, "Control aspects of switched reluctance motor drives," in *IEEE International Symposium on Industrial Electronics, 1993. Conference Proceedings (ISIE'93)*, 1993, Budapest, pp. 296-300.

[7] A. A. Goldenberg, I. Laniado, P. Kuzan, and C. Zhou, "Control of switched reluctance motor torque for force control Applications," *IEEE Trans. Ind. Electron.*, vol. 41, pp.461-466, Aug. 1994.

[8] H. K. Bae, B. S. Lee, P. Vijayraghavan and R. Krishnan, "A linear switched reluctance motor: converter and control," *IEEE Trans. Ind. Applicat.*, vol 36, pp. 1351-1359, Sep. /Oct. 2000.

[9] W. C. Gan, N. C. Cheung and L. Qiu, "Position control of linear switched reluctance motors for high precision applications," *IEEE Trans. Ind. Applicat.*, vol. 39, pp.1350-1362, Sep. /Oct. 2003.

[10] B. Y. Ma, T. H. Liu and W. S. Feng, "Modeling and torque pulsation reduction for a switched reluctance motor drive system," in *Proceedings of the 1996 IEEE IECON 22nd International Conference on Industrial Electronics, Control, and Instrumentation*, 1996, vol. 1, pp. 72-77.

[11] W. C. Gan, K. K. Chan, G. P. Widdowson and N. C. Cheung, "Application of linear switched reluctance motors to precision position control," in *First International Conference on Power Electronics Systems and Applications*, 2004, pp. 254-259.

[12] W. C. Gan, N. C. Cheung and L. Qiu, "Short distance position control for linear switched reluctance motors: a plug-in robust compensator approach," in *IEEE Industry Applications Conference*, 2001, vol. 4, pp. 2329-2336.

[13] G. Ellis, *Control System Design Guide: A Practical Guide,* Elsevier Academic Press, 2004.

VIII. BIOGRAPHIES

Shi Wei Zhao received the B.Sc. degree from Central South University, Changsha, China, the M.Sc. degree from South China University of Technology, Guangzhou, China, in 2000 and 2003, respectively. He is currently pursuing the Ph.D. degree in the Department of Electrical Engineering, Hong Kong Polytechnic University, Kowloon, Hong Kong. His main research interests are motion control and machine drives.

Norbert C. Cheung obtained his BSc, MSc, and PhD from the University of London, University of Hong Kong, and University of New South Wales in 1981, 1987, and 1995 respectively. His research interests are motion control, actuators design, and power electronic drives. He is now working in the Department of Electrical Engineering of the Hong Kong Polytechnic University.

Wai-Chuen Gan received the B.Eng degree (with first-class honors and the academic achievement award) in electronic engineering and the M.Phil. and Ph.D. degrees in electrical and electronic engineering from the Hong Kong University of Science and Technology, Hong Kong, China, in 1995, 1997 and 2001, respectively. From 1997 to 1999, he was a Motion Control Application Engineer at ASM Assembly Automaton Ltd, Hong Kong, China. He rejoined the same company in 2002, and is responsible for the development of the digital motor drivers. His current research interests include robust control of ac machines, power electronics, design and control of linear switched reluctance motors, and control of steeping motors via interconnection and damping assignment.